ELSEVIER

Journal of Contaminant Hydrology 43 (2000) 271–301

JOURNAL OF Contaminant Hydrology

www.elsevier.com/locate/jconhyd

Heuristic space–time design of monitoring wells for contaminant plume characterization in stochastic flow fields

Hubert J. Montas [a], Rabi H. Mohtar [b,*], Ahmed E. Hassan [c], Farqad A. AlKhal [d]

[a] *Biological Resources Engineering, University of Maryland, College Park, MD 20742, USA*
[b] *Agricultural and Biological Engineering Department, Purdue University, West Lafayette, IN 47907, USA*
[c] *Desert Research Institute, University System of Nevada, Las Vegas, NV 89119, USA*
[d] *Kuwait Institute for Scientific Research, Kuwait City, Kuwait*

Received 15 January 1999; received in revised form 5 October 1999; accepted 14 December 1999

Abstract

An optimization methodology for designing groundwater quality monitoring networks applicable to stochastic flow fields is presented and evaluated. The approach sets itself apart from previous techniques by incorporating the time dimension directly into the objective function. This function is extremized using a directed partial enumeration strategy guided by physical considerations related to transport processes. The result is a set of monitoring well locations and a sampling schedule that minimizes plume characterization error while satisfying constraints on the maximum number of wells and allowable number of active wells. The method is evaluated using hypothetical plumes with varying degrees of heterogeneity. Results indicate that the proposed approach is successful in generating near-optimal sampling networks that satisfy all imposed constraints. Monitoring networks with as little as three active wells and a total of 12 wells are found to provide adequate plume characterization for low toxicity contaminants.

Keywords: Heuristic space–time design; Wells; Stochastic flow fields

* Corresponding author. Tel.: +1-765-494-1791; fax: +1-765-496-1115.
E-mail address: mohtar@ecn.purdue.edu (R.H. Mohtar).

0169-7722/00/$ - see front matter
PII: S0169-7722(99)00108-4

1. Introduction

Groundwater is an important natural resource that is exploited throughout the world as a source of domestic and irrigation water. The focus of groundwater investigation has traditionally been on quantification of this resource, but increasing detections of toxic contaminants during the past two decades, including plant nutrients, pesticides, bacteria, non-aqueous phase liquids (NAPLs), heavy metals and radionuclides have shifted this focus towards assessment and protection of groundwater quality as well as prevention, remediation and containment of contamination. The United States Environmental Protection Agency (US EPA), for example, under the Clean Water Act (CWA) currently requires local water utilities to design and implement Well-Head Protection Programs (WHPP) aimed at preventing contamination of the resource. Water providers are required to delineate well capture zones, inventory existing and potential contamination sources within these zones and develop contingency plans incorporating remedial and/or containment measures in the event that contamination would occur. Detection and characterization of contaminated subsurface areas are crucial prerequisites to the implementation of remediation strategies and are typically performed by monitoring groundwater over a network of sampling wells. The design of such networks must consider the natural heterogeneity of the subsurface, aquifer flow characteristics, the presence of potential sources of contamination (e.g., landfills, chemical storage facilities) as well as budgetary constraints. A large body of literature exists proposing different approaches for designing groundwater quality monitoring networks. Andricevic (1996) pointed out that these approaches can in general be based on geostatistical methods (e.g., Carrera et al., 1984; Rouhani, 1985; Rouhani and Hall, 1988; McLaughlin and Graham, 1986), optimization methods (e.g., Olea, 1984; Hsueh and Rajagopal, 1988; Hsu and Yeh, 1989; Loaiciga, 1989; Andricevic, 1990; Hudak and Loaiciga, 1992), methods based on extensive simulation (e.g., Massmann and Freeze, 1987; Meyer and Brill, 1988), or the transfer function method (e.g., Andricevic and Foufoula-Georgiou, 1991).

Monitoring network design is often formulated mathematically as an optimization problem in which an objective function is to be minimized or maximized over a given search space subject to a set of constraints (Loaiciga et al., 1992). The ultimate objective of the design process is generally to minimize the total cost of the system, which includes: (1) installation, operation and maintenance costs; (2) the environmental cost associated with non-detection of the contaminant; and (3) the costs incurred by over-designing or under-designing remediation or containment systems due to inaccurate plume characterization. However, for simplicity, objective functions are most often linked to surrogate goals such as: (1) minimizing the error variance of Kriged concentrations at unmonitored locations (Ben-Jamaa et al., 1995; Lee and Ellis, 1996); (2) minimizing the undetected contaminant mass (Mahar and Datta, 1997); (3) maximizing the number of detections (Meyer and Brill, 1988; Meyer et al., 1994; Storck et al., 1997); (4) maximizing model discrimination (Knopman and Voss, 1991); or (5) maximizing a weighted sum of sub-objective functions including areal coverage and monitoring value (Hudak et al., 1995). A common constraint imposed on the design is to set a

maximum total cost for the physical network, which is often replaced by a constraint on the maximum number of wells to install and use.

The search space for optimization generally consists of two- or three-dimensional space, but seldom includes time. Loaiciga et al. (1992) suggested that time may be important in changing the objectives of monitoring from contaminant detection to plume characterization and back to detection in response to the results of sample analyses. This is, however, a relatively coarse delineation of time effects, which does not deal specifically with the effects of contaminant transport dynamics on network design. Grabow et al. (1993) evaluated the effects of the time at which samples were taken and of the density of the well network on the accuracy of plume characterization using data from two existing sites. Their results indicated that because of the dispersive spreading of the plume with time, it was possible to use a network of lower density, without loss of accuracy, if characterization was to be performed later after the release of a contaminant. They used this information to design networks for snapshots of the plume, but did not provide a methodology for merging the resulting networks into a single design that would be applicable at multiple times and provide a consistent characterization accuracy. Knopman and Voss (1991) recognized the importance of consecutive sampling times on the characterization of contaminant plume dynamics. They developed not only monitoring networks, but also a set of sampling schedules indicating which wells to sample at a given time in order to maximize characterization accuracy (or, more specifically, to maximize model discrimination) while minimizing installation and sampling costs. Their results indicate that only a subset of the network (the active wells) needs to be sampled at a given time, and this time-dependent subset essentially tracks the progression of the plume. Sampling the active wells provides accurate characterization of plume dynamics at a lesser cost than if the entire network was sampled each time. The generality of their results was, however, limited by the fact that they were obtained a posteriori for a specific tracer transport experiment and their design networks were essentially geometrically one-dimensional, consisting of rows of wells located at various distances from the injection point. It can be expected that a fully two-dimensional network geometry would provide equal accuracy, but with a smaller total number of wells through elimination of redundancies. In addition, an a priori design methodology is needed so that monitoring networks can be designed and installed prior to a contamination event. Dynamic a priori network design methodologies were proposed by James and Gorelick (1994) and Mahar and Datta (1997) for source identification and plume delineation, respectively. The basic strategy employed in these studies was to incrementally add new wells, over time, to a small existing network. Wells were added where they would provide maximum new information about the contaminant and the addition process was stopped when either a pre-selected accuracy or a cost constraint was reached. Although the design methodology was dynamic in these studies, the resulting networks did not provide a characterization of the dynamics of the contaminant, but only of its extent or source. Characterizing contamination dynamics, as in the work of Knopman and Voss (1991) is, however, very important because the rates of decay, movement and spreading of a plume are all crucial factors in deciding whether or not remedial measures are necessary, where to target them and how to size them. It is therefore clear that there is a need for the development of a priori network design

methodologies that guarantee accurate characterization of contaminant plume dynamics at low cost. The time dimension must be included in the search space used to design such networks and the result should consist of both a set of monitoring wells and a sampling schedule for these wells. Indeed, in this dynamic situation, the issue is not only how often to sample, but also which wells to sample at a given time to maximize accuracy while minimizing costs. The cost minimization objective must then consider both the total number of wells and the number of active wells, which must be minimized conjunctively to ensure both low construction costs and low operational costs.

The objectives of this study are to present a methodology for designing groundwater quality monitoring well networks in space and time and to evaluate the performance of the resulting networks. The network design objective entails both the determination of well locations and of a sampling schedule representing sampling activity for individual wells as a function of time. The goal is to obtain monitoring networks that maximize contaminant plume characterization accuracy with the smallest possible number of active wells and a small total number of wells. The active wells are expected to be a time-dependent subset of the well field that essentially tracks plume progression with time. The objective function proposed in this work is defined in terms of the spatial moments of the contaminant plume and their time evolution. This function is evaluated using hypothetical truth (reference) plumes generated stochastically to permit a priori design based on the physical characteristics of the site under study. The objective function is extremized using a two-step procedure relying on partial enumeration guided by physical principles that avoid the potential of getting trapped in a local minimum. The proposed methodology is applied to the generation of well networks and sampling schedules for two hypothetical situations.

The proposed objective function for contaminant plume characterization and its associated constraints are presented in Section 2.1. The method used for evaluating the objective function is presented in Section 2.2. The procedure used to extremize this function and the search space over which optimization is performed are discussed in Section 2.3. Section 3 presents the application of the proposed approach to transport scenarios in two-dimensional, horizontal, heterogeneous conductivity fields. The summary of the work and the concluding remarks are presented in Section 4.

2. Methodology

The monitoring system is developed by considering the movement of a conservative contaminant in a heterogeneous flow field caused by spatial variability in the porous medium hydraulic conductivity. It is assumed that the flow is steady and there is no change in the velocities of groundwater within the time scale of interest. This assumption does not significantly deviate from reality since groundwater levels and piezometric head change very slowly with time such that it is safe to deal with steady flow conditions. We further assume that a three-dimensional aquifer can be replaced by a depth-averaged two-dimensional domain through which simulations can be simplified with minor deviations from reality. As discussed by Hassan et al. (1998), there are situations in which two-dimensional simulations are poor approximations of natural

three-dimensional systems. However, two-dimensional models are of value when studying problems at the regional scale (Dagan, 1986). The regional scale is defined for aquifers whose planar dimension is much larger than the aquifer thickness. In this case, formation properties are averaged over depth and are regarded as functions of the horizontal dimension only (Rubin, 1990). Steady, uniform, and two-dimensional flow prevails at the natural gradient tracer experiment in the sand aquifer that was carried out at the Borden site (Curtis et al., 1986; Freyberg, 1986; Mackay et al., 1986; Roberts et al., 1986; Sudicky, 1986). Freyberg (1986) found that the motion of the plume and its center of mass is essentially horizontal. Barry et al. (1988) also found the assumption of two-dimensional flow to yield good results. In the other, commonly cited, natural tracer test performed at the Cape Cod site, LeBlanc et al. (1991) found that the plume centroid moved vertically downward for only a small distance and this enabled Deng et al. (1993) to reproduce the field spatial moments using a two-dimensional stochastic model. The Columbus site (Boggs et al., 1992) has a horizontal dimension about 10–100 times larger than the aquifer thickness and as such can also be considered two-dimensional. It is therefore clear that two-dimensional models can be very useful tools to study and predict contaminant behavior in natural aquifers and can be used to design monitoring well networks do detect and characterize plume spreading and evolution in regional aquifers.

2.1. Definition of the objective function

The overall objective of the design process is to determine an optimal set of groundwater monitoring well positions (network) and a well activity schedule such that arbitrary contaminant plumes evolving in the vicinity of these wells are characterized with maximum accuracy at minimum cost by sampling the design network according to its design schedule. The cost constraint in this objective is linked to installation, maintenance, sampling, analysis and labor costs, which are in turn proportional to the total number of wells in the network and the number of active wells determined by the sampling schedule. For this reason, the cost minimization objective is replaced by a minimization of the total number of wells and a constraint on the maximum number of active wells. Actual cost may, however, be used if actual figures of individual costs are known for a given location and an example of this is presented later in the paper. In addition, the objective of maximizing plume characterization accuracy is replaced by a minimization of plume characterization error, which is equivalent but mathematically simpler.

Let $X_i = (x_i, y_i, t_i)$ denote the coordinates of a point i in two-dimensional space and time and $V = \{X_1, X_2, \ldots\}$ be the set of potential space–time sampling points for the zone to be monitored. Define M^t as the set of sampling locations at a given time t (active wells) and M as the union of all sampling locations over the duration of monitoring T (well network). The design problem is to identify the subset M of V with the property that: (1) monitoring groundwater over the elements of M (through M^t) minimizes contaminant plume characterization error, $e(M)$; (2) M has minimal cardinality; and (3) the cardinality of the set of active wells $M^t \subset M$ at any sampling time t is smaller or equal to a preset maximum value, N_{aw}.

Parts 1 and 2 of the design problem are in opposition to one another since decreasing $|M|$ generally leads to increases in $e(M)$ and vice versa. The problem formulation is therefore ill-posed, and solving it requires, first, that it be reformulation in a well-posed form. This can be achieved by either: (1) using a composite objective function that, for example, is a weighted linear combination of $|M|$ and $e(M)$; or (2) using either $|M|$ or $e(M)$ as the objective function and a constraint on the maximum value of $e(M)$ or $|M|$, respectively. The second approach is adopted here because of the lack of information on appropriate combinations of $|M|$ and $e(M)$. An investigation of possible combinations based on total cost will be pursued in future work. The proposed objective is:

$$\text{Minimize: } e(M), \quad M \subset V$$
$$\text{Subject to: } |M| \le N_{\max}$$
$$\text{and: } M^t \le N_{aw}, \quad \forall t \in [0,T]$$

where $N_{\max}$ is the maximum total number of wells

In this work, contaminant plumes are characterized at any time t by the mass of contaminant that they contain, the position of their centroid in the x and y directions and their extents in both directions. These characteristics are described by the zeroth, first and second centered spatial moments of the plume (Grabow et al., 1993), which are defined by:

$$\mu_0(t) = \int_A nc(x,y,t)\,\mathrm{d}A$$

$$\mu_{1x}(t) = \frac{\int_A nxc(x,y,t)\,\mathrm{d}A}{\int_A nc(x,y,t)\,\mathrm{d}A}; \qquad \mu_{1y}(t) = \frac{\int_A nyc(x,y,t)\,\mathrm{d}A}{\int_A nc(x,y,t)\,\mathrm{d}A}$$

$$\mu_{2x}(t) = \frac{\int_A nx^2 c(x,y,t)\,\mathrm{d}A}{\int_A nc(x,y,t)\,\mathrm{d}A} - \mu_{1x}^2(t);$$

$$\mu_{2y}(t) = \frac{\int_A ny^2 c(x,y,t)\,\mathrm{d}A}{\int_A nc(x,y,t)\,\mathrm{d}A} - \mu_{1y}^2(t)$$

where $c(x,y,t)$ is contaminant concentration at point (x,y) and time t, n is the porosity of the aquifer, and the integration is performed over all space (area in 2D and volume in 3D). The plume characterization error at time t: $e_t(M^t)$ is defined in terms of the difference between spatial moments calculated based on concentrations sampled over M (identified by a circumflex, e.g., $\hat{\mu}_{2y}(t)$) and the true moments of the reference concentration plume (calculated over V). Since M^t consists of a set of discrete locations, the integrals in the above equations are replaced by sums, for example:

$$\hat{\mu}_0(t) = \frac{1}{\Delta M^t} \sum_{i=1}^{|M^t|} c_i(t)$$

where M^t is the set of active wells at time t, ΔM^t is the spatial density of the active well network (wells/m^2) and $c_i(t)$ is the concentration of contaminant in groundwater sampled at the ith element of M^t.

Since there is more than one spatial moment that needs to be reproduced by the sampling network, the plume characterization error at time t is defined as the maximum of the absolute values of the relative errors of estimated plume moments at that time:

$$e_t(M^t) = \max\left[|e_0(M^t)|,|e_{1x}(M^t)|,|e_{1y}(M^t)|,|e_{2x}(M^t)|,|e_{2y}(M^t)|\right]$$

where

$$e_0(M^t) = \frac{\hat{\mu}_0(t) - \mu_0(t)}{\mu_0(t)}$$

$$e_{1x}(M^t) = \frac{\hat{\mu}_{1x}(t) - \mu_{1x}(t)}{\sqrt[3]{\mu_{2x}(t)}} \qquad e_{1y}(M^t) = \frac{\hat{\mu}_{1y}(t) - \mu_{1y}(t)}{\sqrt[3]{\mu_{2y}(t)}}$$

$$e_{2x}(M^t) = \frac{\sqrt[3]{\hat{\mu}_{2x}(t)} - \sqrt[3]{\mu_{2x}(t)}}{\sqrt[3]{\mu_{2x}(t)}} \qquad e_{2y}(M^t) = \frac{\sqrt[3]{\hat{\mu}_{2y}(t)} - \sqrt[3]{\mu_{2y}(t)}}{\sqrt[3]{\mu_{2y}(t)}}.$$

Note that the relative error on the centroid is scaled by the plume extent rather than the true centroid position to provide independence from the origin of the coordinate system used to calculate the moments (the plume extent is estimated as three times its standard deviation; for a gaussian plume, this would encompass 99% of the contaminant mass — Fischer et al., 1979). Also, the error on the second moment is expressed directly in terms of plume extent, which is more physically meaningful than μ_2. Several alternative error estimators and combinations (to form e_t) were tested prior to selecting those presented above. The alternatives for individual moments included absolute errors, absolute values of absolute errors, relative errors with the first moment divided by μ_1 and relative errors on μ_2 rather than its square root. Combinations included the sum of individual moment errors, the sum of the squares of individual moment errors and the maximum of individual moment errors. In most cases, a single moment was found to dominate the error for nearly all sampling times and the corresponding error estimators were discarded. The final selection of estimators, presented above, was found to give the most variability in dominant moment error over time and to have a straightforward physical interpretation.

The contaminant plume characterization error of the network for a monitoring duration of T is selected to be: $e(M) = \max_t[e_t(M^t)]$, $t \in [0,T]$. This equation is also the objective function to be minimized subject to the constraints on $|M|$ and $|M^t|$ stated previously. Here, some alternatives were again evaluated prior to selecting the above formulation. The mean characterization error from 0 to T and the square root of the mean of characterization errors squared (RMSE) from 0 to T were considered, but discarded as objective functions for design. Minimizing the mean error, for example, would not guarantee excellent performance of the designed network for arbitrary sampling times unless the standard deviation of errors was also minimized or at least

constrained. The RMSE, on the other hand, combines mean error and standard deviation in the form of a single euclidean error measure (RMSE = $\sqrt{\sigma_e^2 + \bar{e}^2}$; Neter et al., 1990), but was judged more difficult to interpret, and, hence, less suitable for design than the maximum error. The mean and standard deviation of characterization errors, while not used for design, are used later in this work as a posteriori indicators of the performance of networks designed based on the maximum error.

The use of the zeroth to second spatial moments may slightly limit the degree of characterization provided by the designed system. Errors in the third and fourth spatial moments, which describe the asymmetry (skewness) and peakedness (kurtosis) of a spatial distribution (Kendall and Stuart, 1977) can be easily added to the objective function. This was not pursued in this study because evaluating these moments significantly increases computational time and because a network that accurately reproduces the lower spatial moments is expected to provide at least fair estimates of asymmetry and peakedness if they become necessary.

2.2. Evaluation of the objective function

In practical problems of monitoring network design, the true contaminant plume is the unknown, and, therefore, it is impossible to determine the characterization error associated with a design M a priori. This difficulty can be dealt with by basing the design on one or more hypothetical truth (or reference) plume(s) generated by a transport model (Massmann and Freeze, 1987). Uncertainties associated with the highly heterogeneous nature of subsurface hydraulic properties have made Monte Carlo simulation a primary technique for generating reference and test plumes used in monitoring well network design (Loaiciga et al., 1992). In many instances, individual realizations are used for the design (e.g., Mahar and Datta, 1997; Storck et al., 1997), but this is computationally expensive. Basing the design on the ensemble-averaged plume, which represents the expected value of contaminant concentration throughout the zone being modeled, is expected to be much more efficient from computational and cost perspectives, and is the approach used in this work. Further efficiency improvements can also be achieved by using accurate perturbation-based or volume-averaged equations for the simulations as demonstrated by Hassan et al. (1997, 1998). Network design methods based on ensemble statistics (in the time domain) were also proposed by Massmann and Freeze (1987) and Morisawa and Inoue (1991).

The truth plumes used for evaluating the proposed objective function during the design process are obtained in a manner similar to the work by Hassan et al. (1997). We briefly review the approach employed to generate independent plume realizations. It is assumed that the studied domain is rectangular and inscribed into the horizontal plane with constant head along the boundaries located up-gradient and down-gradient from the contaminant source and no flow across the other two boundaries. The conductivity at any point in the domain is described by $K = K_G e^f$ where K_G is the constant geometric mean conductivity and f is the log conductivity deviation: $f = \log(K/K_G)$. The log conductivity deviation is assumed to form a statistically homogeneous, isotropic, and second-order stationary random field. This allows the description of this heterogeneity

by a limited number of parameters, namely the $\log K$ variance: σ_f^2, correlation scale: λ and lag covariance function: $\mathrm{Cov}_f(s)$, where s is the spatial lag. We assume an exponential distribution for the spatial correlation of the $\log K$ field: $\mathrm{Cov}_f(s) = \sigma_f^2 e^{-s/\lambda}$. Random conductivity fields that respect these statistics are generated using a spectral method (Hassan et al., 1997). Given these settings, the flow equations, represented by the mass balance equation and Darcy's law, are solved using a block-centered finite difference method. The partial differential equation governing the groundwater flow is discretized and locally applied for each block of the discretized conductivity field. This yields a set of linear equations with a size equivalent to the number of nodes representing the studied domain. These equations are directly solved for the nodal heads at the centers of the domain blocks. In order to compute the groundwater flux at the interface between two adjacent blocks, the inter-block conductivity is obtained by harmonic averaging the conductivity of the two blocks. This harmonic average is then multiplied by the head gradient across the interface to obtain the flux and then divided by the porosity to obtain the velocity field. For more details regarding the solution of the flow equations and the accuracy of the solution in terms of local mass balance, global mass balance, boundary effects, and head and velocity stationarity the reader is referred to Hassan et al. (1998).

Having obtained the velocity field for each realization of the heterogeneous conductivity field, the solution of the transport equation and the spatio-temporal evolution of the concentration field are obtained by employing a random walk, particle tracking technique. The random walk method provides a suitable technique that does not require any grid for computations, except the grid that was originally used to obtain the velocity field. In addition, numerical dispersion, which is a common problem with finite difference and finite element methods for the solution of the advection–dispersion equation, does not exist in the particle tracking method (Kinzelbach and Ackerer, 1986). Results of Moltyaner et al. (1993, Fig. 12) have shown that the random walk method completely eliminates numerical dispersion. This is important because numerical dispersion causes artificial spreading of contaminant plumes in excess of that which results from physico-chemical processes and therefore produces inaccurate predictions of the second spatial moment of these plumes. The idea of the particle tracking method is to replace the initial contaminant mass with a large number of particles, NP, of equal mass, m, and trace these particles in the space–time domain. The initial concentration, C_0, considered deterministic and constant, is given by $C_0 = (\mathrm{NP}m)/(n\Omega)$, where Ω is the area of the initial solute pulse. Ahlstrom et al. (1977) suggest that 10^3–10^4 particles may be sufficient for a one-component model. We used 2500 particles in all the transport simulations performed in this study. At each time step, the concentration distribution is approximated as

$$C(x,t) = \sum_{\mathrm{np} \in \mathrm{NP}} m\big(X_{\mathrm{np}}(t),t\big)\eta\big(x - X_{\mathrm{np}}(t)\big)$$

where np = 1, 2, 3, …, NP is the particle index, NP is the total number of particles used to simulate the continuous solute mass, $X_{\mathrm{np}}(t)$ is the position of the $\mathrm{np}^{\mathrm{th}}$ particle at time t, which was initially at $X_{\mathrm{np}}(0)$, $m(X_{\mathrm{np}},t)$ is the mass associated with that particle, and $\eta(x)$ projects the contribution of all particles in a small neighborhood around point x to

the concentration value at that point. The most simple choice for η is a box function with value $1/a$ inside an area a centered at x and zero, otherwise. In this work, concentration values were projected to the blocks used in the finite difference discretization of the flow equation. The positions of the particles are updated at each time step according to the random-walk equation (Kinzelbach, 1988; Tompson and Gelhar, 1990)

$$X_{t+\Delta t} = X_t + \left[\boldsymbol{V}(X_t,t) + \Delta \cdot \boldsymbol{d}(\boldsymbol{V}(X_t,t))\right]\Delta t + \left[2\boldsymbol{d}(\boldsymbol{V}(X_t,t))\Delta t\right]^{1/2} \cdot \boldsymbol{Z}$$

where $X_{t+\Delta t}$ is the updated position of the particle that was at X_t in the previous time step, $\boldsymbol{V}(X_t, t)$ is the velocity vector at the old position at time t, $\boldsymbol{d}$ is the local scale dispersion tensor, Δt is the time step, and $\boldsymbol{Z}$ is a vector of normally distributed random numbers of zero mean and unit variance.

The particle-tracking experiments are performed in the inner zone of the flow domain that is not affected by the boundaries. The initial pulse is released within this inner core and the simulation is terminated before the plume begins to exit this region. Accuracy and convergence issues pertaining to the solutions of the flow and transport equations are discussed in detail in Hassan et al. (1998). Simulation results obtained on individual realizations at a given time t are then averaged using 1200 realizations to form the ensemble-averaged plume at time t. The succession of ensemble-averaged plumes from time 0 to T forms the time-dependent plume used to evaluate $e(M)$ during the well network design process. One or more realizations can then be used to evaluate the design.

The Monte Carlo approach was used in this work because results were readily available from the previous work of Hassan et al. (1997, 1998) and because, in addition to ensemble-averaged plumes used for design, they provide individual realizations with which to test the network design approach. Ensemble-averaged plumes generated by efficient and accurate perturbation approaches can be used in routine design application of the proposed methodology. An advantage of the Monte Carlo approach, however, is that it can easily incorporate macroscopic trends in the conductivity field induced, for example, by buried rivers. This type of non-stationarity as well as reactive contaminants are readily integrated in the proposed design methodology, but are not performed in this study because of time and space constraints.

2.3. Extremization of the objective function

The extremization of the objective function in most network design problems is difficult because of the large size of the search space (potentially all space and time), the existence of multiple local minima and the integer nature of the problem (Lee and Ellis, 1996). This type of problem can be approached with heuristic optimization algorithms or partial (directed) enumeration techniques. Lee and Ellis (1996) compared several heuristic techniques and suggested that they would be vastly more efficient than complete enumeration in two-dimensional search spaces. A drawback of these techniques, however, is that they do not take advantage of the physical nature of transport processes. This is especially important in the present case in which time is considered and the fact that contaminant plumes spread out with time due to dispersion can be used advantageously during the design process. This type of physical consideration and other

insights of the designer are, however, easily incorporated into partial enumeration strategies (Knopman and Voss, 1991). The proposed extremization technique uses partial enumeration directed by physical and geometric considerations relevant to transport processes in porous media.

The success of enumeration strategies depends strongly on the size of the search space. Since the plumes used in this work are generated based on Finite Difference simulations of transport, the ''expected'' values of contaminant concentration are known only on a grid G with nodes coincident with the centroids of blocks used to discretize the flow domain and with the discrete time values corresponding to time steps of the simulations. The search space is consequently reduced from V (continuous space–time) to G (discrete space–time). Secondly, the ensemble-averaged plume delimits a space–time envelope outside of which the expected contamination is null and therefore does not contribute to characterization (James and Gorelick, 1994). The search space can therefore be reduced to the set of grid nodes S contained within this envelope without loss of information. We have: $M \subset S \subset G \subset V$, and for each time step: $M^k \subset S^k \subset G^k$ in which the superscript k is used to indicate the subset of M, S and G defined at the kth time step. For example, M^k represents the set of active wells at the kth time step and S^k are grid nodes within the plume at that time.

Despite the significant reduction of search space from V to S, the optimization problem is still extremely large and not amenable to full enumeration. For example, selecting six active wells for each of the 10 time steps when S^k consists of a modest 100 nodes would require the generation and testing of 12 billion networks. To curb this combinatorial explosion, the present study combines a partial enumeration aimed at further reducing the search space with a full enumeration over an information-maximizing subset of the resulting reduced, search space. The method is only approximate, but yields excellent results as discussed in the next section. The approach consists of two steps:

$$\begin{aligned} &(1)\ \text{Minimize:} && |M_1|, \qquad M_1 \subset S \\ &\text{Subject to:} && e(M_1) \le e_1 \\ \\ &(2)\ \text{Minimize:} && e(M_2), \qquad M_2 \subset M_1 \\ &\text{Subject to:} && |M_2^k| \le N_{\text{aw}}, \qquad \forall k \in [0, K] \end{aligned}$$

The error level e_1 plays a critical role in this procedure. It is selected to ensure $|M_1| \approx N_{\max}$ and gives an iterative nature to step 1: if $|M_1| \gg N_{\max}$ then e_1 must be increased (i.e., the error criterion should be relaxed by increasing the allowable level 1 error) and step 1 is repeated, otherwise, step 2 will be extremely time consuming and may not fulfil the constraint $|M_2| \le N_{\max}$; if $|M_1| \ll N_{\max}$ then e_1 must be decreased and step 1 is repeated, otherwise, step 2 will not produce a near-optimal network. The procedure can be viewed as the generation of a preliminary network, M_1, that is super-optimal with respect to $e(M)$, but fulfils the constraint on $|M|$ only approximately, followed by a coarsening of this network resulting in M_2 which displays near-optimal characterization error and respects the constraint on $|M^k|$ and expectedly on $|M|$as well. The reason for generating M_1 based on a minimization of $|M_1|$ rather

than $e(M_1)$ is that the former can be performed much more efficiently than the latter as discussed below. Steps 1 and 2 are described in Sections 2.3.1 and 2.3.2.

2.3.1. Determination of M_1

The preliminary network, M_1, is determined by identifying and later merging sub-networks with minimal density (and associated geometry) required to maintain plume characterization error below e_1 from an initial time $t_i = k_i t$ to the end of the transport simulation (K). Advective–dispersive transport of contaminants leads to gradual spreading of solute plumes, which suggests that well density can be decreased away from the source of contamination without severe loss in characterization accuracy (Grabow et al., 1993). For a given plume area, a less dense network contains fewer wells and is therefore less costly to install, maintain and sample, which makes it highly desirable.

To determine M_1, networks with 1, 0.5, 0.2, 0.1, 0.05, 0.02, 0.01, 0.005, 0.002, 0.001 and 0.0005 wells/m^2 are generated and ranked by geometry based on the maximum error that they produce from k_i to K. For each density, a series of periodic unit-cell-based geometries are evaluated (Fig. 1). Unit cells are characterized by their widths in the x and y directions, the number of wells that they contain and the pattern of well positions within them (w_x, w_y, nc and p, respectively). The density d of these cells defines that of

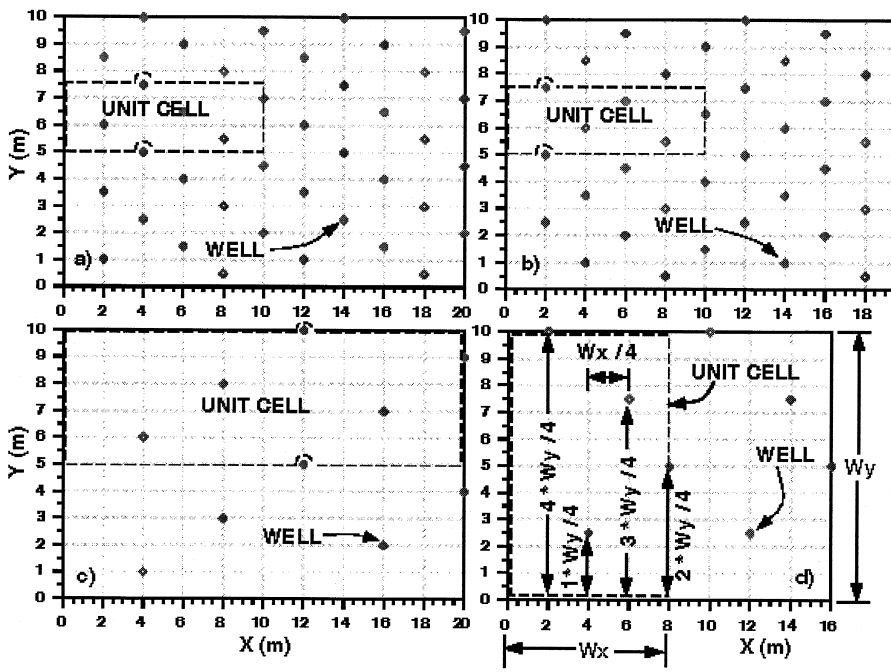

Fig. 1. Examples of well network patterns, geometries and densities: (a) $w_x = 10$ m, $w_y = 2.5$ m, nc = 5, $p = (2, 5, 3, 1, 4)$, $d = 0.2$ well/m^2; (b) $w_x = 10$ m, $w_y = 2.5$ m, nc = 5, $p = (5, 2, 4, 1, 3)$, $d = 0.2$ well/m^2; (c) $w_x = 20$ m, $w_y = 5$ m, nc = 5, $p = (1, 3, 5,2, 4)$, $d = 0.05$ well/m^2; (d) $w_x = 8$ m, $w_y = 10$ m, nc = 4, $p = (4, 1, 3, 2)$, $d = 0.05$ well/m^2.

the network: $\Delta M = d = \mathrm{nc}/w_x w_y$. Cell widths of 0.5–50 m are used with nc = 1 to 5 wells per cell. In each case, nc! geometric patterns are generated to locate wells within the cells based on the permutations of the vector $p = (f_1, \ldots, f_{\mathrm{nc}})$ in which $1 \le f_i \le \mathrm{nc}$, $f_i \ne f_j$ if $i \ne j$, and the position of the ith well in the cell is described by the x and y offsets from the lower left corner: $x_{\mathrm{off}} = iw_x/\mathrm{nc}$ and $y_{\mathrm{off}} = f_i w_y/\mathrm{nc}$.

For each density d and at each time step k, the geometry p providing the smallest maximum characterization error $e_{t,T}$ from k to K is selected to form the preliminary network, $M_{d,p}^{k,K}$. This means that if $M_{d,p}^{k,K}$ is implemented, then the expected characterization error will never exceed $e_{t,T}(M_{d,p}^{k,K})$ from time t to T after the release of a contaminant. A plot of $e_{t,T}$ vs. t for all d can then be used to identify density-error tradeoffs and determine feasible network density transitions with time that respect the constraint e_1 on maximum error. The result of this step is the set of potential sampling wells $M_0 = M_{d_1,p_1}^{k_1,K} \cup M_{d_2,p_2}^{k_2,K} \cup \ldots$ with $e_{t_i,T}(M_{d_1,p_1}^{k_1,K}) \le e_1 \ \forall i$ and $k_{i+1} > k_i$, $d_{i+1} < d_i$, and, therefore, $e_t(M_0) \le e_1$. The indexed time steps identified by k_i in this formulation are those at which the density and geometry of the network can be changed from the pair (d_{i-1}, k_{i-1}) to (d_i, k_i) without increasing characterization error above e_1, as determined from the density-error tradeoff analysis. Next, for each density d_i, the set $M_{d_i,p_i}^{k_i,K}$ is reduced to $M_{d_i,p_i}^{k_i,k_{i+1}} = M_{d_i,p_i}^{k_i,K} \cap S^{k_i,k_{i+1}}$ where $S^{k_i,k_{i+1}}$ is the ensemble-averaged plume envelope between time steps k_i and k_{i+1}. This step does not modify e_t since wells in each $M_{d_i,p_i}^{k_i,K}$ are sampled only between k_i and k_{i+1} (after which wells in $M_{d_{i+1},p_{i+1}}^{k_{i+1},K}$ are sampled and so on). Finally, M_1 is formed by merging the $M_{d_i,p_i}^{k_i,k_{i+1}}$: $M_1 = M_{d_1,p_1}^{k_1,k2} \cup M_{d_2,p_2}^{k_2,k_3} \cup \ldots$, which ensures that $e(M_1) \le e_1$ for all time steps.

A well-sampling schedule can be determined for M_1 based on an arbitrary sampling frequency f_s (e.g., 1 set of samples/week). The sampling frequency is arbitrary because the construction ensures that e_1 is never exceeded irrespective of the specific time at which samples are taken. If sampling is performed at a time t_s corresponding to time step k_s with $k_i < k_s < k_{i+1}$ then the wells to be sampled are determined by $M_1^{k_s} = M_{d_i,p_i}^{k_i,k_{i+1}} \cap S^{k_s}$ where S^{k_s} is the envelope of the ensemble-averaged plume at that time step. The number of active wells at that time is $N_{\mathrm{aw}(1)}^{t_s} = |M_1^{k_s}| < |M_{d_i,p_i}^{k_i,k_{i+1}}| \ll |M_1|$ and will generally depend on sampling time t_s. In addition, $N_{\mathrm{aw}(1)}^{t_s} \le |M_1 \cap S^{k_s}|$ and, hence, not all wells within the plume envelope need to be sampled to meet the characterization accuracy determined by e_1. The well-sampling schedule is then defined as the set of times and corresponding active wells $(t_{si}, M_1^{k_{si}})$ where the sampling times t_{si} are determined from an arbitrarily selected sampling frequency.

The construction process guarantees that $N_{\mathrm{aw}(1)}$ is minimum at any time (i.e., irrespective of sampling frequency), because the sub-networks, $M_{d_i,p_i}^{k_i,k_{i+1}}$, all have the smallest density necessary to maintain e_1. The construction also guarantees that the preliminary well network, M_1, will have a small cardinality since it is the union of minimum density sub-networks. The number of wells $|M_1|$ will be a true minimum if sampling times are selected in such a way that whenever successive sampling times correspond to sub-networks of differing density, there is no overlap between the ensemble-averaged plume envelopes at these times. In other cases, there will be overlap between the lowest density sub-networks merged to form M_1 and this will cause $|M_1|$ to be only a near minimum. Such near minima are accepted in this work because the sampling frequency required to obtain a true minimum is expected to be too low to

properly characterize plume dynamics within a relatively short time (e.g., 1 month) and before it has traveled over a significant distance from its source (e.g., 50 m). Furthermore, the reason for minimizing $|M_1|$ is to permit a nearly full enumeration to be performed in the second part of the design process and a near-minimal $|M_1|$ is sufficient for this process.

2.3.2. Determination of M_2

The final monitoring well network, M_2, is determined by selecting wells from M_1 in such a way that $e(M_2)$ is minimized and the constraint on the number of active wells ($|M_2^k| \leq N_{aw}$) is respected. This is achieved through enumeration of combinations of N_{aw} wells from M_1, which is feasible since $|M_1|$is relatively small. For each time step k, the N_{aw}-combination from $M_1^k = M_1 \cap S^k$ producing the smallest characterization error is selected to form M_2^k. During this process, $|M_2|$ is minimized by maximizing well reuse. For this purpose, the set M_2 is formed in order of increasing k and all wells of M_1^k, which are in the envelope of plumes for time steps 1 to $k-1$, but not in the current $M_2 = M_2^{k_1} \cup M_2^{k_2} \cup \ldots \cup M_2^{k-1}$ are deleted from M_1^j based on position for all times $j \geq k$. Hence, the search space for each M_2^k consists of the current M_2 and the portion of M_1^k that lies within the kth plume envelope, but not in that of previous plumes. This portion of M_1^k is that which adds the most information on the k^{th} plume relative to that which can already be derived from M_2. The use of this heuristic thus decreases computational time, keeps $|M_2|$ small and is not expected to significantly degrade the plume characterization accuracy of the resulting network, especially when a small time step is used in the design process as is the case in this study. Since M_2 is sampled from M_1, which provides very high characterization accuracy (e_1) and has a small cardinality, $|M_1|$, and since M_2 has a smaller cardinality and has the maximum accuracy for a given number of active wells $N_{aw} < N_{aw(1)}$, it is expected that M_2 is at least near optimal for plume characterization.

This construction process minimizes the plume characterization error for a given number of active wells through full enumeration over the reduced search space defined by the well reuse heuristic (reduced from M_1). The use of full enumeration guarantees that global rather than local minima are identified over this search space and, hence, avoids problems related to the non-convexity of the problem. This is an advantage over gradient-based optimization strategies and search algorithms such as Branch and Bound (B&B), which may get trapped in local minima. The process further ensures that the constraint on the number of active wells is satisfied at all times. The sampling schedule for the resulting monitoring well network consists of an arbitrary set of sampling times (possibly based on a constant frequency) and the corresponding active well subsets defined by M_2^k.

If the well reuse heuristic is not used then the search space over which M_2 is developed is richer than each individual $M_{d_i,p_i}^{k_i,k_{i+1}}$ used to form M_1. At any time step k, it contains portions of sub-networks with densities varying from more than that required to meet e_1 to less than that minimal density. Thus, as $N_{aw} \to N_{aw(1)}$, it is guaranteed that $e(M_2) \leq e(M_1)$ where equality corresponds to the worst-case situation: $M_2 = M_1$. Similarly, because of the potential for well reuse across sub-networks, it is guaranteed that $|M_2| \leq |M_1|$. Thus, overall, M_2 is guaranteed to be at least as accurate as M_1 and

have at most the same number of wells as M_1 for the same number of active wells. The well reuse heuristic is not expected to significantly reduce characterization accuracy as discussed above but should significantly decrease $|M_2|$. Thus, it is expected that when the heuristic is used, the maximum error made when sampling M_2 will tend to a value of the order of e_1 as $N_{aw} \to N_{aw(1)}$ but with $|M_2| \ll |M_1|$. In other words, the final networks, M_2, will have accuracies comparable to those of M_1, for the same number of active wells, but will be significantly less costly to build because they contain a smaller total number of wells.

The main reason for forming M_2 is to reduce N_{aw} (i.e., to choose $N_{aw} \ll N_{aw(1)}$), and in so doing, one necessarily has to accept maximum characterization errors larger than e_1. The maximum error is, however, arguably less important to network design than its expected value and standard deviation taken over all potential sampling times. These statistics indicate the expected performance of a well network independently of sampling frequency, whereas, the maximum error may occur only once or twice over all potential sampling times. The standard deviation further provides an estimate of the confidence that the designer can attach to plume characteristics obtained from a single set of samples. Similar to the maximum error, the expected characterization error of M_2 is expected to tend to that of M_1 as $N_{aw} \to N_{aw(1)}$ and to be greater than that of M_1 when $N_{aw} \ll N_{aw(1)}$. These performance statistics are used in this work to evaluate the effect of N_{aw} on the characterization accuracy of the final designs determined by M_2.

Whereas, the expected characterization error (a combined error measure) provides the overall picture of network performance that is important for design purposes, it does not depict the accuracy with which individual plume characteristics are estimated by sampling the network. This is because e_t is a combination of errors on several plume moments and that they are combined using absolute values. Thus, the error cancellations that occur during successive over- and under-evaluations of individual moments are not incorporated in the expected value of e_t. These are important, however, in a real world situation where the dynamics of a plume are evaluated from multiple samples taken at successive times. The mean and standard deviation of errors on individual moments (e_0 to e_{2y}) are therefore used in this work to evaluate the ability of the final design networks, M_2, to characterize the mass, position and extent of a single realization of a contaminant plume.

Finally, we note that the order in which the active sub-networks, M_2^k, are formed may be varied if a pre-specified set of sampling times is provided, but this possibility is not used in the present study. Also, in estimating plume moments from M_2^k (to determine $e_t(M_2^k)$, network density is assumed to be given by: $\Delta M_2^k = n/A^k$ in which the sampled area is approximated by: $A^k = [\max(|x_i^k - x_j^k|) + \min(|x_i^k - x_j^k|)][\max(|y_i^k - y_j^k|) + \min(|y_i^k - y_j^k|)]$ where (x_i, y_i) and (x_j, y_j) are the spatial coordinates of two wells in M_2^k and $i \neq j$.

3. Results and discussion

The proposed monitoring well network design methodology was applied to two hypothetical situations in which a 6×2 m slug of contaminant had been released in an

aquifer resulting in a uniform concentration of 0.4 units (Fig. 2). The two scenarios correspond to different degrees of heterogeneity of hydraulic conductivity: $\sigma_f^2 = 0.15$ and $\sigma_f^2 = 0.40$, and in both cases, $K_G = 2.72$ m/day, $\lambda = 1$ m. The average transport velocity in the x direction was 0.48 m/day (0 in the y direction) and the flow and transport equations were solved on a 0.5×0.5m grid with a time step of 0.5 days. Fig. 2(b) and (c) presents the ensemble-averaged plume for $\sigma_f^2 = 0.40$ at 25 and 50 days, respectively, while results for $\sigma_f^2 = 0.15$ are presented in Fig. 2(d) and (e). An example realization of the hydraulic conductivity field with corresponding transport results are presented in Fig. 2(f), (g) and (h). In all cases, the plume boundary was cut off at a concentration of 0.001 units, which corresponds to 0.25% of the source concentration.

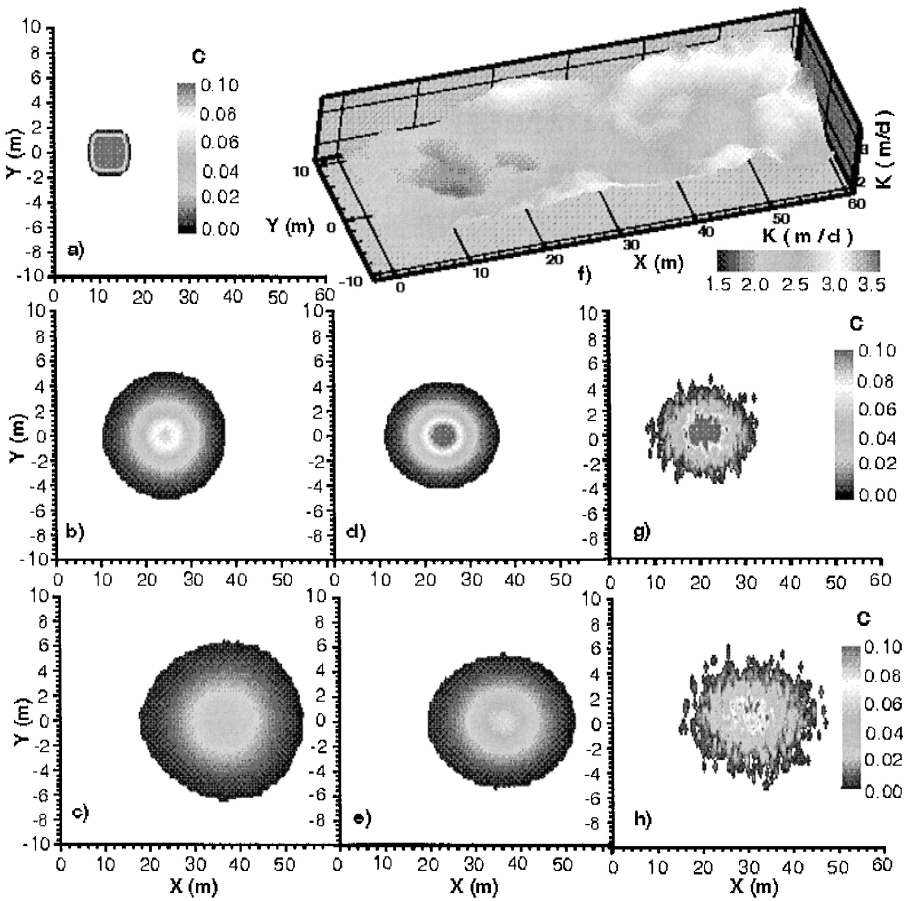

Fig. 2. Plumes used for monitoring network design and testing. (a) Initial condition for transport simulations (slug of contaminant). (b and c) Ensemble-averaged contaminant plume after 25 and 50 days for $\sigma_f^2 = 0.40$. (d and e) Ensemble-averaged contaminant plume after 25 and 50 days for $\sigma_f^2 = 0.15$. (f) Example random conductivity field generated with $\sigma_f^2 = 0.15$. (g and h) Contaminant plume in random field (f) after 25 and 50 days.

Considering a 1 mg/l source of trichloroethylene, for example, the cutoff corresponds to 2.5 μg/l, which is slightly below the EPA human health 10^{-6} risk threshold of 2.7 μg/l (Novotny and Olem, 1994). Higher source concentrations can be adopted without invalidating the design methodology by simply lowering the plume cutoff. This, however, increases the computational time necessary for network design because the plume envelope becomes larger.

Results demonstrate that dispersion leads to increases in plume area with time and that a higher variance of the conductivity field (i.e., a larger value of σ_f^2) leads to more dispersion of the contaminant and, hence, spatially larger plumes at any given time. One also notes that the single realization of transport is significantly more irregular than the ensemble average and, hence, should be more difficult to characterize. However, neither the ensemble-averaged plume nor the single realization appear strongly asymmetric on the whole or significantly peaked, which suggests that characterization up to the second moment is adequate.

The constraint on maximum total number of wells is selected as $N_{max} = 50$ for this example, and the maximum number of active wells N_{aw} is given values of 3–11. Hence, a preliminary network, M_1, with approximately 50 wells and a preliminary sampling schedule are generated for each of the two heterogeneity scenarios. Then, nine final networks, M_2, each with its own constant number of active wells and sampling schedule are designed from each of the two M_1. The preliminary error level e_1 is set tentatively to 5% and may be revised if $|M_1|$ is significantly different from 50. The results of the systematic investigation of network density and geometry on characterization error (first step in determining M_1) are presented in Fig. 3. A total of 7503 geometries were evaluated for both plumes. In each case, the time step used to evaluate plume characterization errors was 0.5 day, which is the same as that used in the flow and transport simulations. Results indicate that network densities larger than 0.5 well/m^2 yield essentially no error for both plumes (not shown), while densities smaller than 0.005 well/m^2 produce errors greater than 50% for the first 50 days of transport. For a fixed network density, the error is observed to decrease as time increases reflecting the increase in plume dimension. This result is in agreement with those of Grabow et al. (1993). Similarly, at a given time and for a given error level the more dispersed $\sigma_f^2 = 0.40$ plume requires a less dense network than the less dispersed plume. This result appears counter-intuitive at first, but is exactly as expected. Indeed, a more heterogeneous conductivity field causes the plume to be more spread, spatially, at any given time than it is in a less heterogeneous field. Thus, if the plume was to be characterized with equal accuracy by sampling only two wells, for example, then these wells would have to be placed farther apart in the highly heterogeneous field than in the less heterogeneous field. Wells placed farther apart correspond to a lower spatial density of the monitoring network, which is the result obtained herein. Network density would probably have to be increased with conductivity heterogeneity if the objective was to characterize within-plume concentration heterogeneity, but this is not the goal of the present study, which is focused on overall plume characteristics: mass, position, extent and their dynamics.

Fig. 3 is used to determine the sub-network densities and geometries that produce characterization errors below $e_1 = 5\%$. Five breakpoints are identified for both plumes

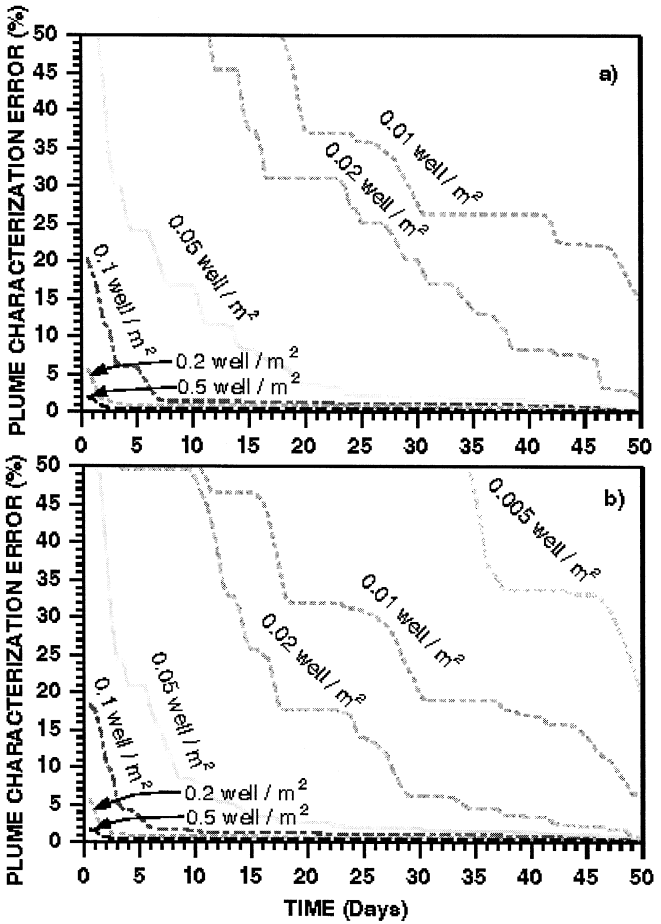

Fig. 3. Evolution of contaminant plume characterization error with time for several network densities (a) $\sigma_f^2 = 0.15$; (b) $\sigma_f^2 = 0.40$.

corresponding to densities of 0.5, 0.2, 0.1, 0.05, and 0.02 well/m^2. The associated sub-network geometries, transition times and contamination envelopes are shown in Figs. 4 and 5(a)–(e). Results clearly illustrate how network density can be decreased away from the source of contamination without loss in characterization accuracy. Density transitions occur earlier for the larger variance plume owing to its faster spread. It is interesting to note that despite the relative symmetry of the contaminant plume with respect to $y = 0$, none of the selected sub-network is symmetrical (although all are regular due to the generation process). This suggests that the enumeration strategy successfully eliminates duplicate information. Indeed, if the concentration is the same at points $(20, -3)$ and $(20,3)$ there is no need to sample both locations (no information is gained by sampling the second point). This result is not necessarily true for a single realization (much more irregular), but in as much as one cannot determine a priori which

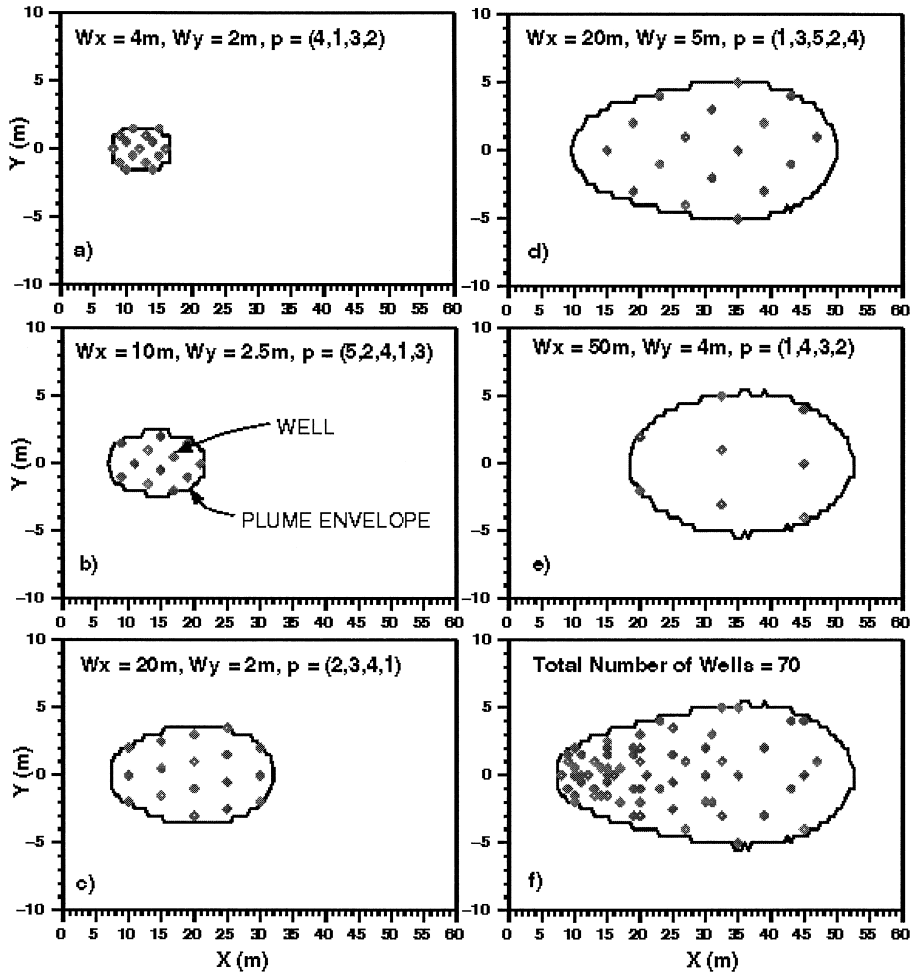

Fig. 4. Selected network densities and geometries for a target error level of 5% when $\sigma_f^2 = 0.15$. (a) Day 0 to 1, $d = 0.5$ well/m^2; (b) day 1.5 to 5, $d = 0.2$ well/m^2; (c) day 5.5 to 18.5, $d = 0.1$ well/m^2; (d) day 19 to 46, $d = 0.05$ well/m^2; (e) day 46.5 to 50, $d = 0.02$ well/m^2; (f) day 0 to 50, merged networks and contamination envelope.

of many equally likely realizations a given field situation corresponds to, the unique well (located at say $(20, -3)$) is equally likely to over-sample as it is to under-sample the plume, leading to a small expected value of the error. This type of error cancellation is reflected in the value of e_t calculated based on the ensemble-averaged plume, but would not be apparent if e_t was calculated for each individual realization and then averaged over their ensemble (or over time) because of the use of absolute values in e_t. Thus, both e_t and error statistics for individual moments (with their signs) are used later to evaluate the performance of the designed networks for a single realization. Asymmetric networks were also obtained by Meyer and Brill (1988) and Meyer et al. (1994) using a

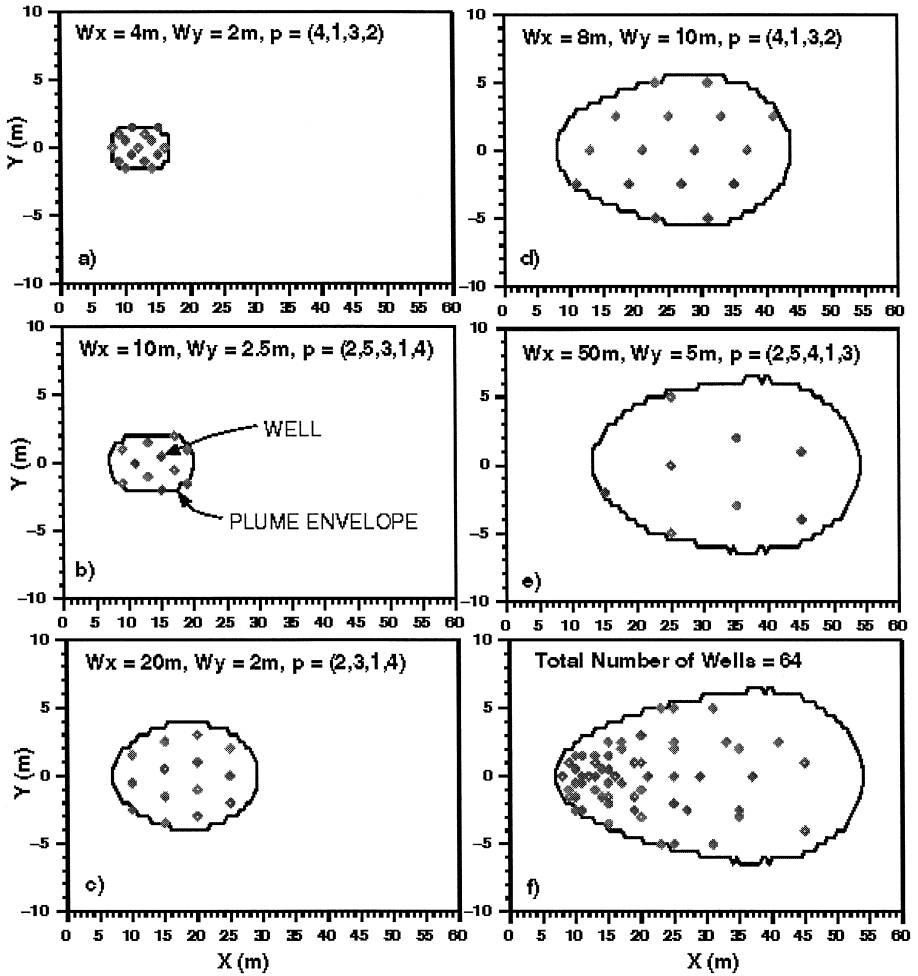

Fig. 5. Selected network densities and geometries for a target error level of 5% when $\sigma_f^2 = 0.40$. (a) Day 0 to 0.5, $d = 0.5$ well/m^2; (b) day 1 to 3, $d = 0.2$ well/m^2; (c) day 3.5 to 13.5, $d = 0.1$ well/m^2; (d) day 14 to 34, $d = 0.05$ well/m^2; (e) day 34.5 to 50, $d = 0.02$ well/m^2; (f) day 0 to 50, merged networks and contamination envelope.

simulated annealing optimization process and Monte Carlo simulations based on the advection–dispersion equation, which suggests that asymmetry is neither an artifact of the optimization method nor of the numerical solution technique used in this study, but a genuine characteristic of the optimal solution to the monitoring well design problem.

The sub-networks presented in Figs. 4 and 5(a)–(e) each contain the minimum number of wells necessary to characterize the plumes with a maximum error of 5%. This number reaches a maximum of 17 for sub-network (d), which also spans the longest range of potential sampling times (approximately 3 weeks). There is a significant degree of overlap between successive sub-networks and, therefore, the preliminary network,

M_1, formed by merging them will display only near minimality of $|M_1|$. True minima can, however, be obtained if the sampling frequency is low as discussed previously. For $\sigma_f^2 = 0.15$, a true minimum is obtained by sampling once every 3 weeks for a total of 6 weeks (three samplings) with M_1 formed by merging sub-networks (a) and (d) only, for a total of 31 wells (the nearly overlapping wells at (16,0) of (a) and (15,0) of (d) are replaced by a single well at either (15.5,0) or (15,0)). Similarly, merging (a) and (d) and sampling every 2 weeks for 4 weeks provides a true minimum of $|M_1| = 30$ for $\sigma_f^2 = 0.40$ (after replacing wells at (12,0) and (13,0) with a single well). These true minima are not used further in this work because they require a specific sampling frequency and contain too many active wells (15–17).

Figs. 4(f) and 5(f) present the preliminary sampling networks, M_1, obtained by super-imposing the sub-networks described above. These networks contain 70 and 64

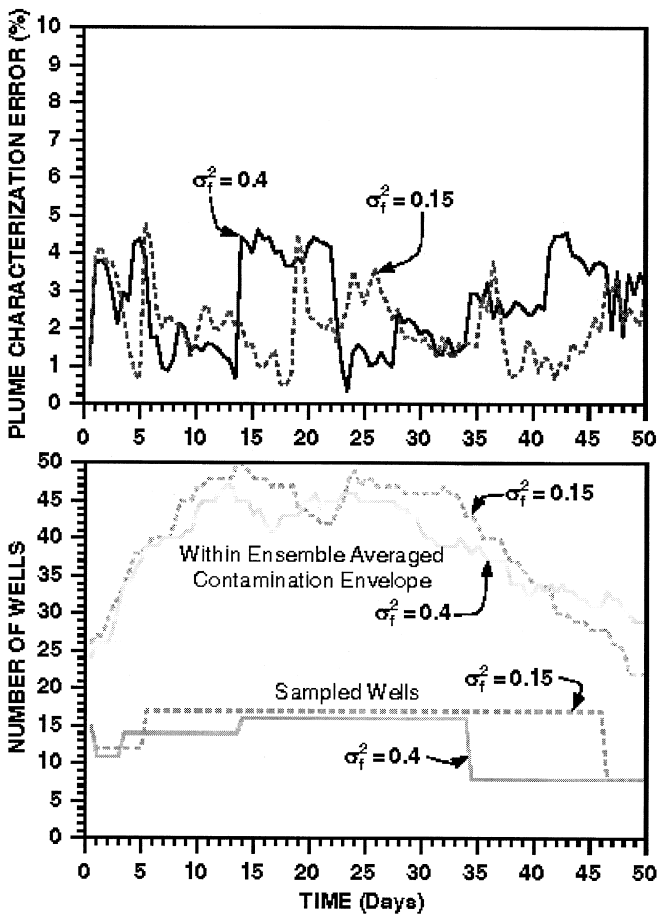

Fig. 6. Plume characterization error and number of wells as a function of time when sampling the merged well networks of Figs. 4 and 5. (a) Maximum contaminant plume characterization error; (b) Number of wells sampled and total number of wells within the contamination envelope.

wells, which is judged to be close enough to $N_{max} = 50$ that $e_1 = 5\%$ need not be modified. Some of the wells are very close to one another suggesting that they can be replaced by a single well to reduce $|M_1|$. This would, however, reduce the richness of the search space used to develop M_2 and, hence, is not performed here. Fig. 6(a) shows the actual characterization error occurring when wells are sampled according to M_1 and demonstrates that this error is always less than $e_1 = 5\%$. The expected characterization error over all time steps and its standard deviation are 2.10% and 0.95%, respectively, for $\sigma_f^2 = 0.15$ and 2.68% and 1.19%, respectively, for $\sigma_f^2 = 0.40$.

Fig. 6(b) shows the number of wells actually sampled (active) and total number of wells within the ensemble average plume envelope as a function of time. The schedule of M_1 requires that 16–17 wells be sampled most of the time, which corresponds to sub-networks (d) of Figs. 4 and 5, and is judged to be excessive. The figure indicates that up to 50 wells are included within the plume envelope during the monitoring process and, therefore, it is quite possible that sampling M_1 with a different schedule and smaller number of active wells will lead to similar characterization at significantly less cost. This is the purpose of the second step of the design process, which leads to the final monitoring networks, M_2.

Final monitoring networks, M_2, generated by resampling M_1 with 3, 6, 9 and 11 active wells are presented in Figs. 7 and 8 for the two ensemble-averaged plumes. The number of active wells is constant in each one of these networks developed using the

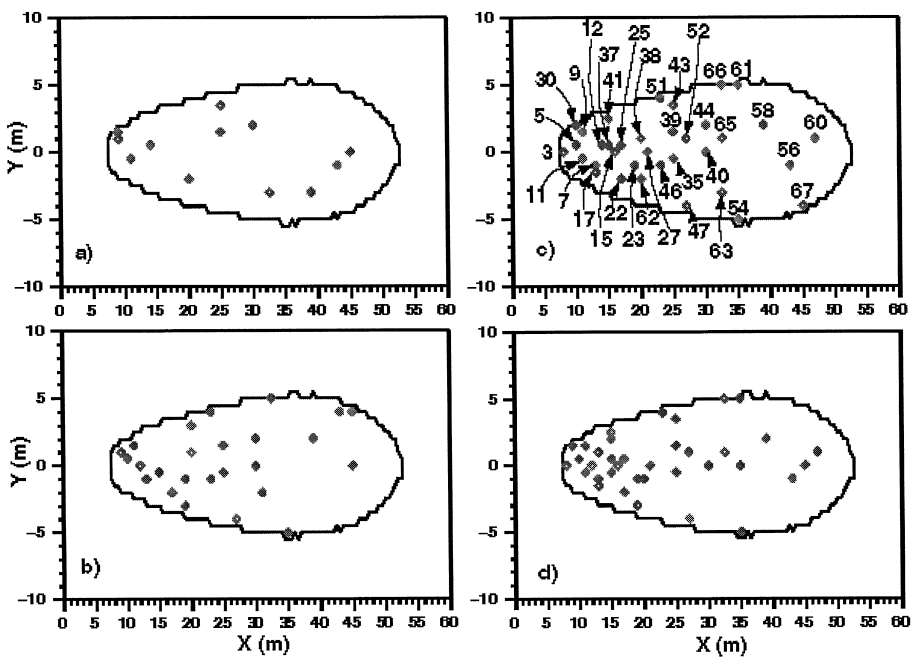

Fig. 7. Final groundwater monitoring well networks, M_2, designed for $\sigma_f^2 = 0.15$ with (a) three active wells (total of 12 wells); (b) six active wells (total of 25 wells); (c) nine active wells (total of 35 wells); (d) 11 active wells (total of 36 wells).

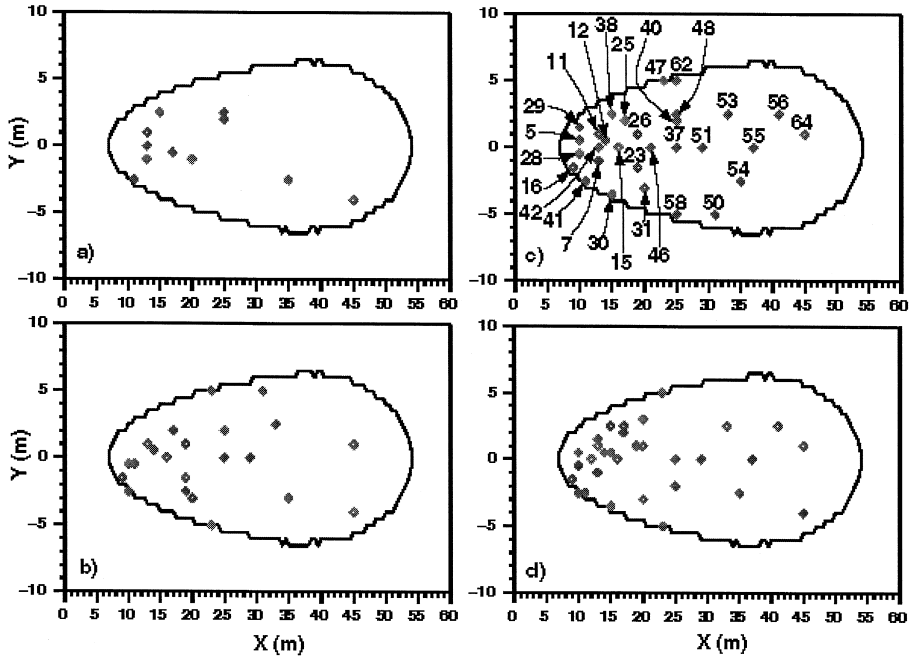

Fig. 8. Final groundwater monitoring well networks, M_2, designed for $\sigma_f^2 = 0.40$ with (a) three active wells (total of 11 wells); (b) six active wells (total of 22 wells); (c) nine active wells (total of 30 wells); (d) 11 active wells (total of 31 wells).

full enumeration strategy with well reuse as described previously, with a time step of 0.5 day. They therefore support a maximum sampling frequency of twice per day. The networks are once again non-symmetric and well density decreases away from the contaminant discharge point. The total number of wells increases from approximately 10 with three active wells to three times that value with 11 active wells and meets the allowable maximum of 50.

Error statistics from sampling the final networks developed with 3–11 wells are presented and compared to those of M_1 in Fig. 9. The mean characterization error (over half-day time steps) and its variance generally decrease as the number of active wells is increased from 3 to 11 indicating progressively better characterization. These trends are modeled using exponentials of the form $\alpha e^{\beta N_{aw}}$ with least square parameters given in Fig. 9. Fluctuations of the expected errors around the exponentials are attributed to the limits imposed on the search spaces used to form M_1 and M_2. These limits include the use of periodic unit cells, discrete (rather than continuous) network densities and the well reuse heuristic. It is expected that increasing the number of densities used to form M_1, using aperiodic unit cells or forming M_2 from all wells within the plume envelope would reduce these fluctuations. These alternatives would, however, significantly increase computational time or lead to final networks with a larger total number of wells. The magnitude of fluctuations gives an indication of the distance between the designed networks and optimal networks. The error for optimal networks is expected to have the

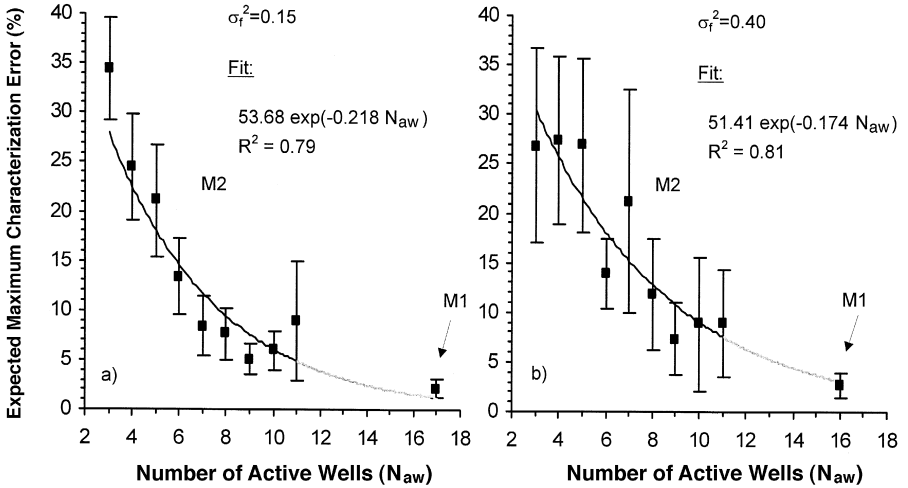

Fig. 9. Error statistics of final monitoring well networks, M_2 as a function of the number of active wells. (a) $\sigma_f^2 = 0.15$; (b) $\sigma_f^2 = 0.40$. Error bars represent one standard deviation.

same trend seen in Fig. 9, but the corresponding error decay curve would pass through the minima of the data values shown in the figure. The fact that fluctuations about the exponentials are generally small (less than 5%) therefore suggests that the designed networks are close to optimal. The nearness to optimality is seen to depend on N_{aw} and σ_f^2. The deviation is often larger in the more heterogeneous conductivity field and, in this case, networks designed with three, six and nine active wells provide the best expected plume characterization performance (expected errors of 27%, 14% and 8%, respectively). Network designed with seven and nine active wells provide the best expected performance for the less heterogeneous plume (expected errors of 8% and 5%, respectively). A sampling schedule for the network with nine active wells, which performed very well for both plumes, is developed later in this paper.

The error decay exponentials in Fig. 9 were obtained by fitting data values obtained with 3–11 active wells. These curves extrapolate almost exactly to the characterization error provided by the preliminary networks, M_1. This result demonstrates the asymptotic nature of the process used to develop M_2, even when the well reuse heuristic is applied, as discussed earlier: $e(M_2) \rightarrow \approx e(M_1)$ as $N_{aw} \rightarrow N_{aw(1)}$. In other words, the well reuse heuristic does not significantly degrade plume characterization accuracy.

A relatively simple tradeoff analysis can be used to demonstrate the dependence of network installation and sampling costs on the desired plume characterization accuracy and to evaluate the cost of the final network in relation to that of the preliminary networks. The cost of installation of a single well is assumed to be US$400 and that of sampling and analysis is assumed to be US$300 per well-sample. These values were obtained from Massmann and Freeze (1987) and cross-checked with a private consultant in northern Indiana. Fig. 10 shows the cost–accuracy tradeoff curves of the design networks for the two heterogeneity scenarios assuming a sampling frequency of once per week (eight sets of samples for a monitoring period of 50 days). The monitoring cost

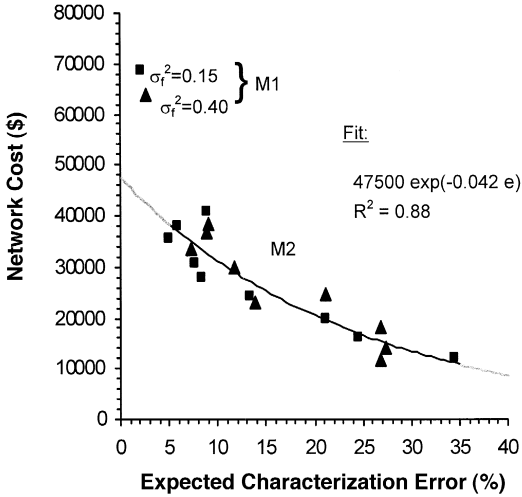

Fig. 10. Cost–accuracy tradeoff curve for the final networks, M_2, compared to the preliminary networks, M_1.

decreases as the allowable error increases, as expected, but does not appear to be significantly affected by the degree of heterogeneity of the subsurface medium. The expected increase in cost (or decrease in economy) with an increase in network accuracy was also reported by Morisawa and Inoue (1991). The lack of effect of heterogeneity is due in part to the fact that, whereas, the lower heterogeneity plume requires a smaller number of active wells to achieve a given characterization accuracy (compare Fig. 9(a) and (b)), it generally requires a larger total number of wells (compare Figs. 7 and 8). In the case of nine active wells, for example, the characterization errors are 5% and 8% for $\sigma_f^2 = 0.15$ and 0.40, respectively, but the corresponding total number of wells are 35 and 30, respectively (Ben-Jamaa et al. (1995) also found an increase in characterization error with media heterogeneity for a constant number of sampling sites). Hence, due to the larger total number of wells, the total cost is larger for the network with greater accuracy. A difference will emerge when monitoring duration is large enough that sampling costs significantly exceed building costs and in this case networks for the lower heterogeneity environment will turn out to be less expensive for a given error level, as one would intuitively expect.

Monitoring M_2 using its design schedule of well activity is obviously less expensive than sampling all wells in the network. For the network with nine active wells ($\sigma_f^2 = 0.15$, expected error = 5%), for example, the total number of wells is 35 and monitoring once a week over all of these wells yields a cost of US$98,000, which is more than two and a half times the US$35,600 cost of monitoring only the nine active wells.

The cost–accuracy tradeoff curve obtained by combining results for both degrees of heterogeneity (Fig. 10) is relatively well approximated by an exponential ($R^2 = 0.88$). Extrapolating this curve to the error level provided by M_1 shows that M_2 is expected to provide equal characterization accuracy for approximately US$23,000 less than M_1.

Table 1
Sampling schedule of final network, M_2 with nine active wells when $\sigma_f^2 = 0.15$

Sampling date (day)	Error (%)	Wells sampled
1	4.5	3, 5, 6, 7, 9, 12, 17, 25, 37
8	6.9	5, 12, 17, 22, 23, 25, 38, 41, 46
15	7.3	5, 12, 22, 23, 35, 38, 41, 46, 52
22	3.0	6, 25, 39, 40, 43, 46, 51, 62, 65
29	5.6	7, 23, 43, 44, 46, 47, 52, 62, 65
36	7.0	22, 35, 39, 47, 51, 56, 58, 63, 65
43	2.6	25, 35, 47, 54, 56, 58, 61, 63, 65
50	6.0	38, 47, 54, 56, 58, 60, 63, 65, 66

This cost reduction is due to the fact that M_2 is expected to have a smaller total number of wells than M_1 when they both have the same accuracy (and also the same number of active wells as discussed in relation to Fig. 9). This result supports the hypothesis that the two-step extremization approach used in this study successfully produces final networks, which have both the smallest number of active wells and the smallest total number of wells (and, hence, the lowest cost) necessary to produce a given plume characterization accuracy, or at least, networks which are quite close to these minima.

Results in Figs. 7–9 also indicate that provided one is willing to accept error levels of 30%, then as little as 12 wells can be used with three active wells at any time. This may be quite acceptable if one remembers that the expected error is based on the maximum of absolute values of individual moment errors and, as such, does not reflect error cancellations from successive over- and under-estimation of these moments. The substantial cost savings (the cost is approximately US$13,500 or US$23,000 less than a network producing 5% error) accruing from the installation maintenance and, hence, sampling of this ''smaller'' well field may justify the adoption of the coarser design, especially for low toxicity contaminants where the risk associated with a less accurate characterization is low.

The designed networks include both well positions and a well-sampling schedule, which depends on the set of selected sampling times. Sampling schedules for the networks with nine active wells are presented in Tables 1 and 2 for a sampling

Table 2
Sampling schedule of final network, M_2 with nine active wells when $\sigma_f^2 = 0.4$

Sampling date (day)	Error (%)	Wells sampled
1	8.8	5, 7, 11, 12, 15, 16, 28, 29, 42
8	8.5	7, 11, 12, 16, 23, 26, 31, 38, 46
15	6.1	16, 23, 25, 26, 30, 37, 42, 48, 51
22	11.2	23, 25, 28, 30, 31, 40, 46, 51, 53
29	4.9	7, 23, 31, 40, 47, 50, 51, 53, 54
36	6.6	12, 15, 23, 47, 50, 51, 53, 54, 56
43	3.9	25, 46, 50, 51, 53, 54, 56, 62, 64
50	18.8	26, 37, 46, 50, 53, 54, 55, 56, 64

frequency of once per week. The numerical IDs of the wells to be sampled at each time in those schedules correspond to values presented in Figs. 7(c) and 8(c). The plume characterization error corresponding to each sampling time fluctuates mildly about the expected value. The mean error over these schedules are 5.4% and 8.6% for $\sigma_f^2 = 0.15$ and $\sigma_f^2 = 0.15$, respectively, and are quite close to the expected values of 5% and 8% that would result from sampling twice a day, which is the maximum frequency supported by the design process. Alternative schedules, possibly with unequal intervals can also be derived easily from the design procedure.

The networks designed for the lower variance plume were also applied to the characterization of the single realization shown in Fig. 2(g) and (h). Fig. 11(a) presents the statistics of the maximum moment error as a function of the number of active wells for this case and suggests that the performance of the networks is lower for the single realization than for the ensemble average plume. The mean error decreases as the

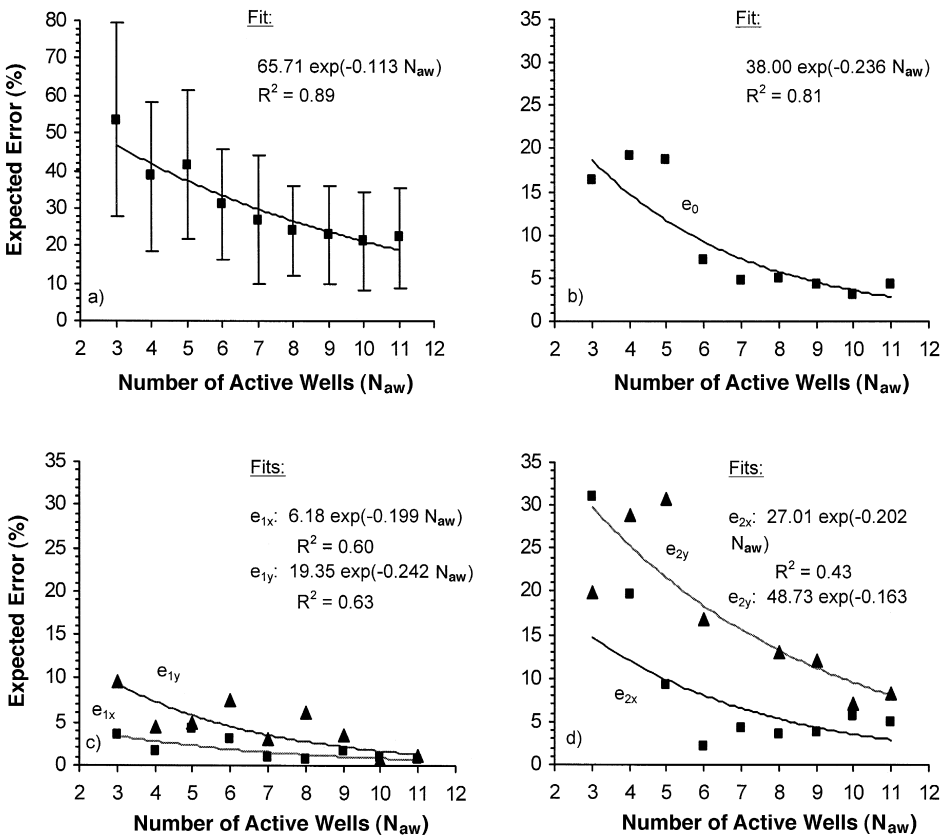

Fig. 11. Plume characterization error statistics for a single realization with $\sigma_f^2 = 0.15$ as a function of the number of active wells for the final monitoring networks. (a) Combined error on all moments, e_t; (b) relative error on the plume mass, e_0; (c) relative error on longitudinal and lateral centroidal position, e_{1x} and e_{1y}; (d) Relative error on longitudinal and lateral plume extent, e_{2x} and e_{2y}. Error bars in (a) represent one standard deviation.

number of active wells is increased but reaches a disappointing minimum of only about 20%. As discussed earlier, the relatively large minimum error in this case is due to the irregularities of the plume and to the use of absolute values in e_t, which does not account for cancellation of over- and under-estimated plume moments when calculated on a single realization. The mean errors for individual plume moments do, however, incorporate such cancellations and provide a more detailed estimate of network performance in a real-world monitoring situation (Fig. 11(b),(c),(d)). The expected errors on individual moments decrease as the number of active wells is increased. Expected errors on all but the second transverse moment have values below 6% whenever more than six active wells are used. The error on the second transverse moment is less or equal to 13% when more than seven active wells are used. It should be noted that although the mean error on the latter moment is generally larger than that on other moments, it is not always the largest at a given time. For example, in the case of nine active wells, the largest error is that on the mass, longitudinal centroidal position, lateral centroidal position, longitudinal extent and lateral extent 34%, 2%, 14%, 12% and 38% of the time, respectively (based on a time step of 0.5 days). It should also be noted that the individual mean errors in Fig. 11 are estimated under the assumption of high-frequency sampling and have relatively large standard deviations. Individual mean errors for lower frequencies are therefore likely to be larger than those presented in the figure. For the sampling schedule presented in Table 1, the mean errors on individual moments are, in order, 4.2%, 2.3%, 2.5%, 6.5% and 10.5% for e_0 to e_{2y}. These results demonstrate the very good performance of the monitoring network with one set of samples taken weekly.

4. Summary and conclusions

A heuristic methodology for designing groundwater quality monitoring well networks in space and time was presented and evaluated. The design objective was to minimize contaminant plume characterization error while satisfying constraints on the maximum number of wells and number of active wells. The objective function was defined in terms of spatial moments of the contaminant plume. A Monte Carlo technique was used to generate the truth plumes that were used to evaluate the objective function. The objective function was extremized using a two-step process relying on a directed enumeration strategy. The results of the design procedure were sets of sampling well positions with associated sampling schedule.

Two ensemble-averaged test plumes and a single realization were used to demonstrate and evaluate the methodology. The proposed design approach generated near-optimal non-symmetric well networks in which sampling density decreased with distance from the point of contaminant release. The mean characterization error decreased as the number of active wells increased and reached a value of 5% to 9% depending on hydraulic conductivity variance at nine active wells. It was suggested that networks with as little as three active wells (total of 12 wells) can give adequate plume characterization for low toxicity contaminants at small cost. Characterization errors for a single realization were higher than those of the ensemble-averaged plume, but followed the same trend with respect to the number of active wells. Expected errors calculated for

individual moments, however, demonstrated the accuracy of the designs in this approximation of real-world conditions.

The proposed methodology is easily extended to non-stationary conductivity fields, reactive contaminants, sampling schedules with unequal time intervals and characterization of plume skewness and peakedness. Future work will focus on evaluating composite objective functions, comparing present results with those of alternate optimization strategies, validating the approach for reactive contaminants, evaluating results at larger scales and testing the methodology on time-dependent flow fields and alternative contaminant release modes. These goals of future work are particularly applicable to the design of well networks used to monitor the progress of bioremediation activities. A long-term goal of the project is to investigate the possible existence of a ''universal'' optimal network geometry and sampling schedule applicable to arbitrary degrees of heterogeneity and contamination scenarios.

References

Ahlstrom, S.W., Foote, H.P., Arnett, R.C, Cole,C.R., Serne. R.J., 1977. Multicomponent mass transport model: theory and numerical implementation (discrete-parcel-random walk version), Rep. BNWL-2127, Battelle Pacific Northwest Lab., Richland, WA.

Andricevic, R., 1990. Cost-effective network design for groundwater flow monitoring. Stochastic Hydrol. Hydraul. 4 (1), 27–41.

Andricevic, R., 1996. Evaluation of sampling in the subsurface. Water Resour. Res. 32 (4), 863–874.

Andricevic, R., Foufoula-Georgiou, E., 1991. A transfer function approach to sampling network design for groundwater contamination. Water Resour. Res. 27 (10), 2759–2769.

Barry, D.A., Coves, J., Sposito, G., 1988. On the Dagan model of solute transport in groundwater: application to the Borden site. Water Resour. Res. 24 (10), 1805–1817.

Ben-Jemaa, F., Marino, M.A., Loaiciga, H.A., 1995. Sampling design for contaminant distribution in lake sediments. J. Water Resour. Plann. Manage. — ASCE 121 (1), 71–79.

Boggs, J.M., Young, S.T., Beard, L.M., Gelhar, W., Rehfeldt, K.R., Adams, E.E., 1992. Field study in a heterogeneous aquifer: 1. Overview and site description. Water Resour. Res. 28 (12), 3218–3291.

Carrera, J., Usunoff, E., Szidarovszky, F., 1984. A method for optimal observation network design for groundwater management. J. Hydrol. 73, 147–163.

Curtis, G., Roberts, P., Reinhard, P.V., 1986. A natural gradient experiment on solute transport in a sand aquifer: 4. Sorption of organic solutes and its influence on mobility. Water Resour. Res. 22 (13), 2059–2068.

Dagan, G., 1986. Statistical theory of ground water flow and transport; pore to laboratory, laboratory to formation, and formation to regional scale. Water Resour. Res. 22 (9), 120S–134S.

Deng, F.W., Cushman, J.H., Delleur, J.W., 1993. A Fast Fourier transform stochastic analysis of the contaminant transport problem. Water Resour. Res. 29 (9), 3241–3247.

Fischer, H.B., List, E.J., Koh, R.C.Y., Imbereger, J., Brooks, N.H, 1979. Mixing in Inland and Coastal Waters. Academic Press, New York, NY.

Freyberg, D.L., 1986. A natural gradient experiment on solute transport in a sand aquifer: 2. Spatial moments and the advection and dispersion of nonreactive tracers. Water Resour. Res. 22 (13), 2031–2046.

Grabow, G.L., Mote, C.R., Sanders, W.L., Smoot, J.L., Yoder, D.C., 1993. Groundwater monitoring network design using minimum well density. Water Sci. Technol. 28 (3–5), 327–335.

Hassan, A.E., Cushman, J.H., Delleur, J.W., 1997. Monte Carlo studies of flow and transport in fractal conductivity fields: comparison with stochastic perturbation theory. Water Resour. Res. 33 (11), 2519–2534.

Hassan, A.E., Cushman, J.H., Delleur, J.W., 1998. A Monte Carlo assessment of Eulerian flow and transport perturbation models. Water Resour. Res. 34 (5), 1143–1163.

Hsu, N.S., Yeh, W., 1989. Optimum experimental design for parameter identification in groundwater hydrology. Water Resour. Res. 25, 1025–1041.

Hsueh, Y.W., Rajagopal, R., 1988. Modeling groundwater quality sampling decisions. Groundwater Monit. Rev. 8, 121–134.

Hudak, P.F., Loaiciga, H.A., 1992. A location modeling approach for groundwater monitoring network augmentation. Water Resour. Res. 28 (3), 643–649.

Hudak, P.F., Loaiciga, H.A., Marino, M.A., 1995. Regional-scale ground water quality monitoring via integer programming. J. Hydrol. 164 (1–4), 153–170.

James, B.R., Gorelick, S.M., 1994. When enough is enough: the worth of monitoring data in aquifer remediation design. Wat. Resour. Res. 30 (12), 3499–3513.

Kendall, M., Stuart, A., 1977. The Advanced Theory of Statistics, Vol. 1. 4th edn. MacMillan, New York, NY.

Kinzelbach, W., 1988. The random walk method in pollutant transport simulation. In: Custodio, E., Gurgui, A., Lobo Ferreira, J.P. (Eds.), Groundwater Flow and Quality Modeling. Reidel, Norwell, MA, pp. 227–246.

Kinzelbach, W., Ackerer, P., 1986. Modelisation du transport de contaminant dans un champ d'ecoulement non-permanent. Hydrogeologie 2, 197–206.

Knopman, D.S., Voss, C.I., 1991. Sampling design for groundwater solute transport: tests of methods and analysis of Cape Cod Tracer test data. Water Resour. Res. 27 (5), 925–949.

LeBlanc, D.R., Garabedian, S.P., Hess, K.H., Gelhar, L.W., Quadri, R.D., Stollenwerk, K.G., Wood, W.W., 1991. Large-scale natural gradient tracer test in sand and gravel, Cape Cod, Massachusetts: 1. Experimental design and observed tracer movement. Water Resour. Res. 27 (5), 895–910.

Lee, Y.M., Ellis, J.H., 1996. Comparison of algorithms for nonlinear integer optimization: application to monitoring network design. J. Environ. Eng. 122 (6), 524–531.

Loaiciga, H., 1989. An optimization approach for groundwater quality monitoring network design. Water Resour. Res. 25, 1771–1782.

Loaiciga, H.A., Charbeneau, R.J., Everett, L.G., Fogg, G.E., Hobbs, B.F., Rouhani, S., 1992. Review of ground-water quality monitoring network design. J. Hydraul. Eng. 118 (1), 11–37.

Mackay, D.M., Freyberg, D.L.P., Roberts, V., Cherry, J.A., 1986. A natural gradient experiment on solute transport in a sand aquifer: 1. Approach and overview of plume movement. Water Resour. Res. 22 (13), 2017–2029.

Mahar, P.S., Datta, B., 1997. Optimal monitoring network and ground-water-pollution source identification. J. Water Resour. Plann. Manage. 123 (4), 199–207.

Massmann, J., Freeze, R.A., 1987. Groundwater contamination form waste management sites: the interaction between risk-based engineering design and regulatory policy: 1. Methodology. Water Resour. Res. 23 (2), 351–367.

McLaughlin, D., Graham, W., 1986. Design of cost-effective programs for monitoring groundwater contamination. IAHS Publ. 158.

Meyer, P., Brill, E.D.Jr., 1988. A method for locating wells in a groundwater monitoring network under conditions of uncertainty. Water Resour. Res. 24 (8), 1277–1282.

Meyer, P., Valocchi, A.J., Eheart, J.W., 1994. Monitoring network design to provide initial detection of groundwater contamination. Water Resour. Res. 30 (9), 2647–2659.

Moltyaner, G.L., Klukas, M.H., Wills, A.C., Killey, W.D., 1993. Numerical simulation of Twin Lake natural-gradient tracer tests: a comparison of methods. Water Resour. Res. 29 (10), 3433–3452.

Morisawa, S., Inoue, Y., 1991. Optimum allocation of monitoring wells around a solid-waste landfill site using precursor indicators and fuzzy utility functions. J. Contam. Hydrol. 7, 337–370.

Neter, J., Wasserman, W., Kutner, M.H., 1990. Applied Linear Statistical Models. 3rd edn. Irwin, Boston, MA.

Novotny, V., Olem, H., 1994. Water Quality: Prevention, Identification and Management of Diffuse Pollution. Van Nostrand-Reinhold, New York, NY.

Olea, R.A., 1984. Sampling design optimization for spatial functions. Math. Geol. 16 (4), 365–391.

Roberts, P.V., Goltz, M.N., Mackay, D.M., 1986. A natural gradient experiment on solute transport in a sand aquifer: retardation estimates and mass balances for organic solutes. Water Resour. Res. 22 (13), 2047–2058.

Rouhani, S., 1985. Variance-reduction analysis. Water Resour. Res. 21, 837–846.
Rouhani, S., Hall, T.J., 1988. Geostatistical scheme for groundwater sampling. J. Hydrol. 103, 85–102.
Rubin, Y., 1990. Stochastic analysis of macrodispersion in heterogeneous porous media. Water Resour. Res. 26 (1), 133–141.
Storck, P., Eheart, J.W., Valocchi, A.J., 1997. A method for the optimal location of monitoring wells for detection of groundwater contamination in three-dimensional heterogeneous aquifers. Water Resour. Res. 33 (9), 2081–2088.
Sudicky, E.A., 1986. A natural gradient experiment on solute transport in a sand aquifer: spatial variability of hydraulic conductivity and its role in dispersion process. Water Resour. Res. 22 (13), 2069–2082.
Tompson, A.F.B., Gelhar, L.W., 1990. Numerical simulation of solute transport in three-dimensional, randomly heterogeneous porous media. Water Resour. Res. 26 (10), 2541–2562.